Electrodeposition of Amorphous Matrix Ni-W/W_p Composites

By

Donald R. Jenket II

SUBMITTED TO THE DEPARTMENT OF MATERIALS SCIENCE AND ENGINEERING IN PARTIAL FULFILLMENT OF THE REQUIREMENTS FOR THE DEGREE OF

BACHELORS OF SCIENCE IN MATERIALS SCIENCE AND ENGINEERING AT THE MASSACHUSETTS INSTITUTE OF TECHNOLOGY

MAY 2005

[June 2005]

Signature of Author: _____

Department of Materials Science and Engineering
May 13, 2005

Certified by: _____

Christopher A. Schuh
Assistant Professor of Materials Science and Engineering
Thesis Supervisor

Accepted by: _____

Donald R Sadoway
John F. Elliott Professor of Materials Chemistry
Chair, Undergraduate Thesis Committee

Electrodeposition of Amorphous Matrix Ni-W/W_p Composites

By

Donald R. Jenket II

SUBMITTED TO THE DEPARTMENT OF MATERIALS SCIENCE AND ENGINEERING IN PARTIAL FULFILLMENT OF THE REQUIREMENTS FOR THE DEGREE OF

BACHELORS OF SCIENCE IN MATERIALS SCIENCE AND ENGINEERING AT THE MASSACHUSETTS INSTITUTE OF TECHNOLOGY

MAY 2005

ABSTRACT

An amorphous Ni-W alloy matrix was incorporated with W particulate through two types of electrodeposition. The plating bath for the electrodeposition contained nickel sulfate, sodium tungstate, sodium citrate, ammonium chloride, and a variable amount of 1μm tungsten particulate ranging in concentration from about 5g/L to 15g/L.The first method was electrodeposition with only moderate stirring of the plating bath. The second method had a forced flow of solution on the substrate via a pump. The results showed incorporation in both methods, but the flowed method resulted in more incorporation. The amount of incorporation increased with the amount of particulate in solution until a limit that lies somewhere between 10g/L and 15g/L of particle concentration. At this point, the incorporation became hindered by the excess amount of particulate in solution. It was also shown that an increase of particulate concentration caused more voids in the material, and the flowed method caused less voids than the normal method. A tapering in the amount of incorporation between the substrate side and the surface side of the deposit was observed; the area close to the substrate had a higher incorporation than the area near the surface. Hardness testing showed mechanical property differences through the thickness of the deposit with the area near the substrate being softer than the area near the surface. Compression testing showed an increase in the strain and a decrease in the stress before failure, suggesting an improvement in ductility.

Thesis Supervisor: Christopher A. Schuh
Title: Assistant Professor of Materials Science and Engineering

Abstract:

An amorphous Ni-W alloy matrix was incorporated with W particulate through two types of electrodeposition. The plating bath for the electrodeposition contained nickel sulfate, sodium tungstate, sodium citrate, ammonium chloride, and a variable amount of 1μm tungsten particulate ranging in concentration from about 5g/L to 15g/L.The first method was electrodeposition with only moderate stirring of the plating bath. The second method had a forced flow of solution on the substrate via a pump. The results showed incorporation in both methods, but the flowed method resulted in more incorporation. The amount of incorporation increased with the amount of particulate in solution until a limit that lies somewhere between 10g/L and 15g/L of particle concentration. At this point, the incorporation became hindered by the excess amount of particulate in solution. It was also shown that an increase of particulate concentration caused more voids in the material, and the flowed method caused less voids than the normal method. A tapering in the amount of incorporation between the substrate side and the surface side of the deposit was observed; the area close to the substrate had a higher incorporation than the area near the surface. Hardness testing showed mechanical property differences through the thickness of the deposit with the area near the substrate being softer than the area near the surface. Compression testing showed an increase in the strain and a decrease in the stress before failure, suggesting an improvement in ductility.

Background:

Ballistic superiority is a crucial part of any military tactics. It is often the case that technological superiority is the deciding factor in battles. In particular, armor piercing ballistics are those responsible for the destruction of the fierce battle tanks in today's world arsenals. In order to make a better armor piercing material, the mechanics of the interaction between the penetrator and the target must be understood. Penetration depth can be determined by the following equation,

$$P = aL\sqrt{\frac{\rho_p}{\rho_t}}e^{-\left(\frac{2S}{\rho_p v^2}\right)}$$

(Andrews, pg 43) where P is the penetration depth, a is a function of the penetrator length/diameter ratio, L is the length of the penetrator, ρ_p is the density of the penetrator, ρ_t is the density of the target, S is a measure of target resistance, and v is the impact velocity.

It is shown here that the desired material property in the penetrator material is density: the higher the density of the penetrator, the greater the penetration distance. Therefore, a desirable material for armor piercing ballistics has the highest density possible. However, this is not the only important material property. The deformation behavior of the penetrator upon impacting a target will also determine its effectiveness. There are currently two major types of armor piercing materials: tungsten heavy alloy (WHA) and depleted uranium (DU). WHA fails through what is commonly referred to as "mushrooming." When a penetrator impacts a target, there is a plastic deformation that results in an increase in flow stress due to work hardening. This increase in flow stress is

partially countered by a decrease in flow stress due to thermal softening. When thermal softening does not overcome the increase in flow stress due to work hardening, mushrooming occurs. This results in the energy being radially expended to increase the penetration cavity. In contrast, the thermal softening does overcome the increase in flow stress from work hardening in DU, resulting in adiabatic shearing, which is also known as "self-sharpening." In this material, the energy is focused on axial penetration rather than racial expansion. Figure 1 illustrates how the two different materials would react upon impact. A self-sharpening material is superior since it concentrates more of its energy towards penetration rather than radial expansion of the penetration cavity. DU seems to be an excellent armor piercing material since it self-sharpens and has a high density. However, DU is only 40% less radioactive than natural uranium, making it a health risk. . Therefore, an alternative material that is dense, self-sharpening, and not radioactive would be desirable. One such material that could be used to replace DU is a metallic glass composite. Metallic glasses exhibit shear bands during failure and generally possess a high hardness; they can also be produced without radioactive components. A specific example is a Ni-W amorphous metal alloy that is processed through electrodeposition. This material has already been produced by a number of authors (Yamasaki, "Formation of Ductile Amorphous & Nanocrystalline Ni-W Alloys by Electrodeposition") and the deposition parameters are well known. The problem with this material is that its density is low and it is fairly brittle. As a result, it would likely shatter upon impact with a target. To fix both of these problems, particulates of a ductile metal could be incorporated into the Ni-W amorphous metal alloy during the processing to yield a composite with a higher degree of ductility. If a dense metal were used, such as tungsten, then the resulting

material would have a higher density as well. This metallic glass composite could serve to replace DU if the particulate can be incorporated into the material.

Procedure:

In electrodeposition, two electrodes are placed in a solution of metallic ions. A potential is then applied across the electrodes such that one develops a more positive polarity—the anode—and the other develops a more negative polarity—the cathode, upon which metal ions are reduced to form a solid form. For these experiments, the cathode was a 5 X 2.1cm strip of commercially pure copper, and the anode was pure platinum. The cathode was first placed in an electropolishing solution and electropolished at a current of 3A for approximately 5 minutes. The electropolished substrate was then placed in the deposition solution. This solution was prepared in a 2L beaker and metal salts were added in the following order and masses: 31.54g $NiSO_4$, 92.39g Na_2WO_4, 294.10g $Na_3C_6H_5O_7$, 53.49g NH_4Cl, along with a variable amount of 1μm W particulate. All of the particulate came from the same source and the particle size was nominally 1μm. In this paper, the amount of particulate in solution is always in terms of grams per liter of solution. This solution was then covered to prevent evaporation and placed in an oil bath at 80°C for approximately one hour to allow proper heating of the solution. To keep the particulate from settling at the bottom of the beaker, a stir bar was placed in the bath. The electrodes were then attached to a Dynatronix Pulse Power Supply model PDPR 40-50-100 and were placed in the solution with the substrate, facing the flow induced by the stirring bar. The power supply was set at a constant 2.12A to provide a .2A/cm^2 current density on the

substrate during deposition. The samples were run for approximately 3 hours resulting in a deposition of about 120μm in thickness. This method is shown in Figure 2. Samples containing 5g/L, 7.5g/L, 10g/L, and 15g/L of particulate were made using this method.

Alternatively, a jet electrolyte setup (flow method) was used. This schematic can be seen in Figure 3. A larger 3L bath was used for this method and all components were scaled accordingly to give the same concentrations as before. The substrate was attached to the out-flow tube of a pump so that the substrate was perpendicular to the flow from the tube and roughly 1-2cm from the end of the tube. The pump was hooked up to a variac and the voltage was fixed at 60V during deposition. Samples were made with 5g/L and 7.5g/L of particulate. All samples made for compression and hardness testing were produced by the 5g/L flow method.

A compression sample was prepared in the same manner as the flow method samples, except it was placed in a 30L solution and allowed to run for about 3 days. Only one of these samples was made. From this sample, three compression samples, approximately 1mm tall and 1mm in diameter, were cut for testing.

Cross-sections of the resulting deposits were prepared using traditional metallographic techniques (mounting and polishing). The cross-sections were observed in a Scanning Electron Microscope Leo 438VP (SEM) operating at 20keV in both secondary and backscatter mode. Microhardness tests were conducted on the same cross-sections on a Clark DMHZ at a load of 50g applied for 15 seconds. Qualitative aspects of the failure

mode were determined by bending freestanding samples to failure and observing the fracture surface in the SEM. An Instron machine was used to gather load vs. displacement response at a strain rate of .05mm/second on the compression sample.

Results:

The first samples were made using the normal (non-flowed) method. The least amount of particulate used was 5g/L. Figure 4 shows the cross sectional SEM image of this sample. The particulates appear as bright dots within the film. This image shows incorporation of the W_p throughout the sample. There seems to be an uneven distribution of the particulate, with a higher volume fraction of incorporation at the substrate end than at the surface end. The sample also seems to have separated from the mounting compound at the surface allowing for a partial view of the surface. It appears that the sample is composed of clusters of material that have grown together. Voids develop where these clusters did not grow together completely. These voids are small, but numerous, and are important because they greatly decrease the density and ductility of the material. Figure 5 shows the cross sectional SEM image of a sample with 7.5g/L W_p. This image shows a series of peaks in the sample. Within these peaks is a large amount of W_p that has been incorporated. Between the peaks, a tapering of the W_p from the substrate to the surface is also seen. Voids are also seen in this sample. Figure 6 shows the cross-sectional SEM image of the 10g/L sample. The first noticeable difference between this sample and the others is the increase in size and number of voids. The sample does not appear to be very structurally sound simply due to the large and numerous voids throughout the material.

The surface of the sample also shows that this material probably grew from a coagulation of clusters but there is a greater amount of empty space between the clusters. The incorporation of W_p seems to be consistent with the previous samples. The W_p is seen tapering off towards the surface of the film, but there does not seem to be a greater amount of incorporation of W_p within the material. Figure 7 and Figure 8 show cross-sectional SEM images of the 15g/L sample. The sample is extremely voided and even appears to have voided channels running through it. The incorporation of W_p appears to be less than that of the 10g/L sample and the tapering seems to be absent as well.

In an attempt to improve incorporation, a series of depositions using the flow method were run. Figure 9 shows the cross-sectional SEM image of the 5g/L W_p deposited using the flow method. This image shows a greater incorporation of the W_p than in the normal method with the same amount of W_p. The tapering can still be seen clearly in this sample. Also, there are more voids where the incorporation is high and fewer to none where there is no incorporation. There are a similar amount of voids as compared to the previous method. Figure 10 shows the cross sectional SEM image of the 7.5g/L W_p deposited using the flow method. There is an extremely high amount of incorporation in this sample. The incorporation seems to be homogeneous throughout the thickness of the film but there are many voids and the material looks highly unstable. Cracks can already be seen in the cross-section. This appears to be far too much incorporation of W_p and the sample seems mechanically unsound.

As a preliminary investigation of the failure mode of these materials, fracture surfaces from bending were observed. Figure 11 shows the SEM image of the fracture surface of

the normally deposited 5g/L sample. This image is looking at the fracture at about a 30° angle. The top rough interface is the fracture surface and the smooth and bumpy part below it is the substrate side of the sample. The image clearly shows that the film consists of coagulated clusters. The fracture surface appears to have broken at the interfaces of these clusters. This sample is likely to be structurally unsound and easily prone to fracture. This is due to the brittle-like fracture that occurs at the interfaces of the clusters. Figure 12 shows the SEM image of the normally deposited 5g/L fracture surface. In this image, the view is looking directly down on the fracture surface. It shows that the fracture surface is full of voids. Figure 13 shows the SEM image of the fracture surface of the normally deposited 7.5g/L sample. This image is looking at the fracture surface at about a 30° angle; the lighter portion on top is the fracture surface. The darker portion below it is the substrate side of the film. This image clearly shows the existing interfaces between the clusters of material. The film is full of voids from these interfaces and the sample does not appear to be structurally sound. Figure 14 shows the SEM image of the normally deposited 7.5g/L sample. The view is looking directly down on the fracture surface. It shows that there are still voids in the film.

Figure 15 shows the SEM image of the flow method deposited 5g/L sample. The view is looking at the fracture surface at a slight angle. The bright area is the fracture surface and the dark area below it is the surface side of the film. The image shows many small clusters that have coagulated together with voids between them. Figure 16 shows the SEM image of the fracture surface of a flow method deposited 7.5g/L sample. The image is looking directly down on the fracture surface. This image shows a high degree of void in the fracture surface. The film does not appear to be structurally sound. There is also a

decrease in the sizes of the clusters as the film grew. The substrate side has larger clusters (about 10μm in diameter) than the surface (about 5μm in diameter or smaller).

Vickers hardness testing was performed on a 5g/L flow method deposited sample. Eighteen indents were made at various points along the cross-section; some were taken near the substrate side of the film and others from the surface side of the film. All indents were annotated where they were taken and the hardness found there. Several of the indents had cracks or were not used for lack of a good indentation. Thirteen measurements were judged to be good and were used to get an average hardness of 3.80 MPa. However, the hardness varied throughout the thickness of the film: the film was softer near the substrate side and harder near the surface. At the sites near the substrate, there was a greater incorporation of W_p than at the surface side. Figure 17 shows an indent taken near the substrate side of the film with visible bright dots of W_p included in the indent; the hardness was 1.08 MPa. Figure 18 shows an indent near the surface of the film with almost no incorporation of W_p in the indent; the hardness was 5.55- MPa. The sample also had some interesting failures as shown in Figure 19. In this figure, a crack has propagated almost entirely around the indent. With such a high amount of incorporation, it should fail in a ductile manner, but this crack suggests that there are a lot of voids in this highly W_p incorporated area.

Figure 20 shows the results of two compression tests conducted on the flow deposited 5g/L W_p samples with a comparison to a compression sample with no W_p, just pure amorphous Ni-W matrix. The pure Ni-W showed a higher stress but smaller strain before failure than the two samples with 5g/L W_p. These two samples had a higher strain but

lower stress before failure; there is an increase in ductility of the material when the 5g/L W_p is present. This indicates that the samples with 5g/L W_p are failing by a different mechanism than the pure Ni-W amorphous alloy. Figure 21 shows the compression sample of pure Ni-W amorphous alloy after the compression test. This image shows a brittle failure of the material after compression. Figures 22 and 23 show SEM images of the first compression sample with 5g/L W_p. These images show a somewhat triangle shaped sample that had pieces break off along one of the sides of the triangle. Figure 22 is looking on the side of the sample that did not fail. Figure 23 is looking at a slight angle down on the surface of the sample allowing the area that underwent failure to be seen. The failure area is the rough-looking area at the bottom of the sample. Figures 24 and 25 show SEM images of the second compression sample with 5g/L W_p. Figure 24 shows a corner where failure occurred and a piece of the material almost separated from the bulk of the sample. Figure 25 shows a rotated perspective to show the area of the sample where pieces did separate from the bulk sample. The failure area is the rough area at the bottom of the sample.

Discussion:

The results show that incorporating W_p in an amorphous Ni-W matrix through electrodeposition is possible. The samples seem to grow by the coagulation of clusters. The flow method of deposition is better than the normal method; this method allows for more incorporation of the W_p into a sample. The flow method gives smaller voids for a set amount of incorporation than the normal method of deposition. These reasons make the flow method more desirable during processing. Almost all of the samples demonstrated a tapering of the particulate as the deposition progressed. This was shown by a greater amount of incorporation of the particulate near the substrate and a lessening of the incorporation towards the surface of the film. This does not seem to be due to the diminishing amount of particulate in solution that is being consumed. Another strange phenomenon associated with the amount of particulate incorporation was the frequency and size of the voids. It appears that as the incorporation of the particulate increases, the material becomes more frequented with voids and their size in larger, as well. These two phenomenons, the tapering and the increase in voids with incorporation, could be due to electrical effects during deposition. The electrical conductivity of the W_p could have some effect on how the particulate is incorporated into the matrix and the surrounding area. It appears that the more W_p in the matrix, the more likely voids are to form in that area. This could be due to each particle of W becoming locally favorable for the Ni-W amorphous matrix to grow on, resulting in nucleation of Ni-W matrix from a W particle. Voids are created where theses clusters impinge on each other. More experimentation with the electrical effects would have to be done to confirm how and why these clusters

grow. Using dielectric particles instead of W_p, for example, may help to determine the cluster growth mechanism. The compression test shows an increase in strain and a decrease in stress before failure when compared to the material with no particulate. This shows that the material with W_p incorporated in it has an increase in ductility when compared to the pure Ni-W amorphous alloy. The failure mechanisms should therefore be different and this was shown by the particulate having an effect on the material properties on a macroscopic level. This was also confirmed by the hardness testing where indents that included more particulate were shown to be softer than those without much incorporation.

Conclusions:

The results have shown that there was successful incorporation of W_p into a Ni-W amorphous matrix through electrodeposition. By varying the amount of W_p in the solution and the method of deposition, the extent of incorporation can be tailored. It was shown that as the amount of W_p in solution increase, the extent of incorporation increased to a limit found between 10g/L and 15g/L. In this region of W_p, it appears that further increase of the W_p hinders incorporation. The 15g/L sample had close to the same magnitude of incorporation as the 5g/L when both were deposited in the normal manner. Changing the deposition method to a forced flow method cause further incorporation of the W_p for a set amount of W_p in solution. The 5g/L sample produced by the flow method had more incorporation than the 5g/L sample produced by the normal method. All samples, except those past the limit, demonstrated a tapering in the amount of

incorporation as the film grew; the area of the film close to the substrate is more incorporated than the area near the surface. There are no sudden jumps in the amount of incorporation but instead this progression appears to be a gradual degradation throughout the thickness of the sample. The hardness test confirmed that the film has mechanical properties associated with the tapering effect of the incorporation. It showed that areas near the substrate, with a lot of incorporation, were soft and the areas near the surface of the film, with little to no incorporation, were hard. The samples also showed a correlation between the amount of W_p incorporation and the number and size of voids in that area. All of the samples show that the size and number of voids increase as the amount of W_p incorporated in the film increases. Due to the tapering and this correlation, the voids appear more frequently and in greater sizes near the substrate than the surface since this is where the incorporation was the greatest. The flow method allowed more incorporation per gram of W_p in solution and it also yielded less voiding than the normal method. The 5g/L sample made by the flow method had one of the greatest amount of incorporation while not having as many voids as would be expected if the same amount of incorporation was found in a sample made by the normal method. The flow method is superior since it gave a higher incorporation with not so many voids as the normal method would give. These voids seemed to result from clusters of the material coagulating together and where they did not completely coagulate, there were voids. Fracture surfaces seemed to indicate that these materials were failing along the interfaces of the clusters, meaning that there was little to no effect from the W_p in the material. However, the compression tests showed that these particles are affecting the failure mechanism of the material. The samples with incorporated W_p showed an increase in

strain and a decrease in stress before failure when compared to a pure Ni-W amorphous sample. This indicates an increase in ductility due to the W_p resulting in a more ductile failure.

The two major concerns in the future would be to further study the origin of the tapering phenomenon and the void formations. Future work would include experimentation of the possible electrical effects on the growth of the film to hopefully find a way to completely rid the sample of voids while making the sample homogeneous with W_p incorporation.

References:

Yamasaki, Tohru. "Formation of Ductile Amprpuous & Nanocrystalline Ni-W lloys by Electrodeposition" Plating and Surface Finishing, May 2000, pp. 148-152.

Yamasaki, Tohru. "High-Strength Nanocrystalline Ni-W Alloys Produced by Electrodeposition and their Embrittlement during Grain Growth." Department of Materials Science and Engineering, Faculty of Engineering, Himeji Institute of Technology, 2167 Shosha, Himeji, Hoyogo 671-2201, Japan. Dec 9, 2000 (accepted in revised form).

T. Yamasaki, P. Schlobmacher, K. Ehrlich, Y. Ogino. "Formation of Amorphous Electrodeposited Ni-W Alloys and their Nanocrystallization." Department of Materials Science and Engineering, Faculty of Engineering, Himeji Institute of Technology, 2167 Shosha, Himeji, Hoyogo 671-2201, Japan. Dec 9, 2000 (accepted in revised form).

Andrews, Williams S. "Depleted Uranium on the Battlefield." Canadian Military Journal, Spring 2003.

H. Takeuchi, S. Tamura, Y. Tsunekawa, M. Okumiya. "Application of Electrolyte Jet to Rapid Composite Electroplating." Vol. 20 No. 1Surface Engineering, 2004.

Campaign Against Depleted Uranium. http://www.cadu.org.uk/

Fahey. "Depleted Uranium Presentation." 2003. http://www.nuclearpolicy.org/documents/fahey_jun_14_03.pdf

KnowledgeMed. "DNA Breaks and Repairs." http://galileo3.knowledgemed.com/radiation/radiobiology/dna/dna/slideshow/

United Nations Environmental Programme (UNEP) Statement. "UNEP Recommends Studies of Depleted Uranium in Iraq, 6 April 2003." Document ID 309. Article ID 3952. UNEP Post Conflict Assessment Unit. Press release 6 April 2003. http:/postconflict.unep.ch/actiraq.htm

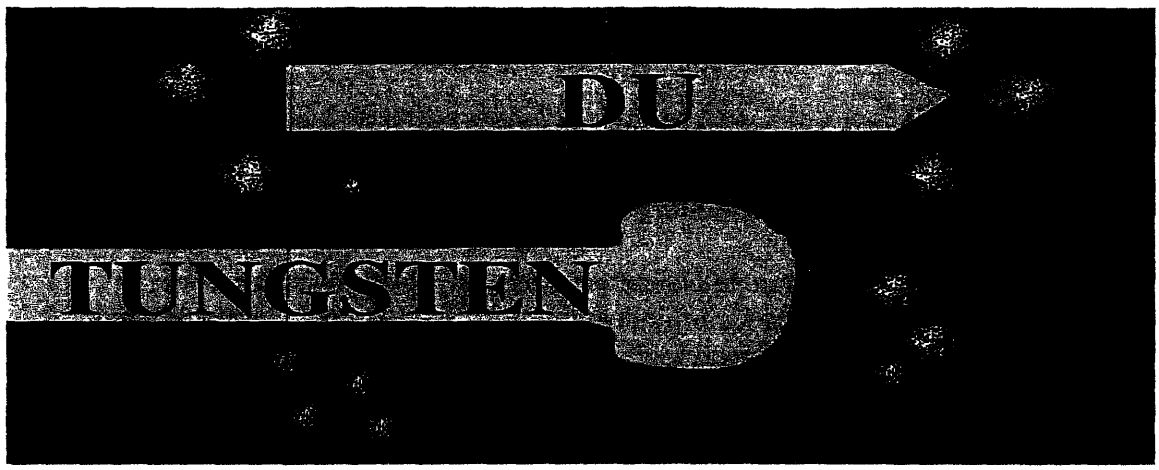

Figure 1: Failure of both penetrator types

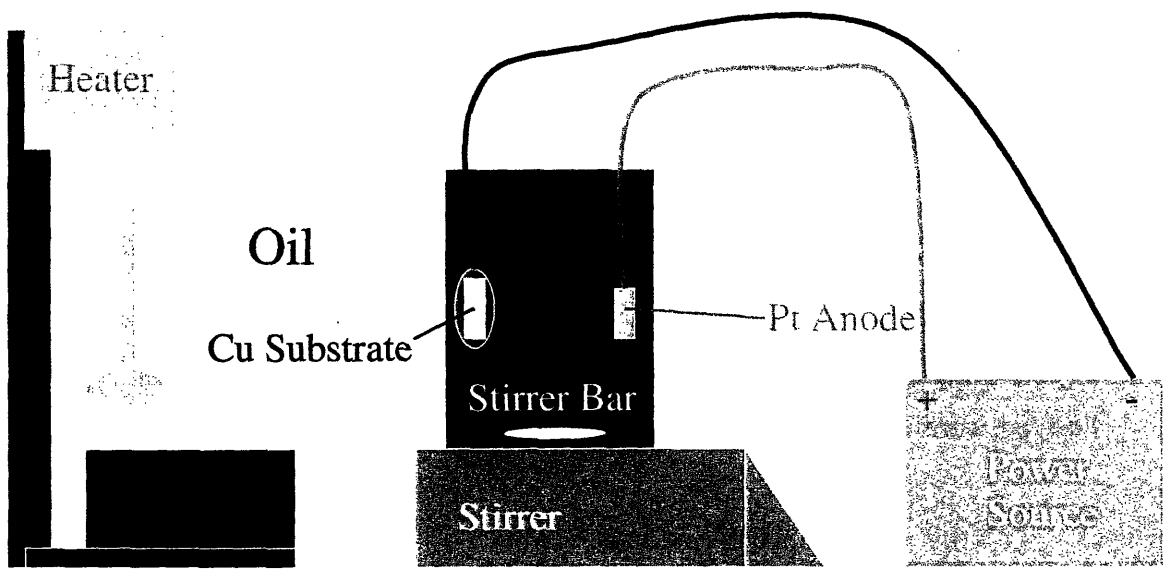

Figure 2: Normal Method Schematic

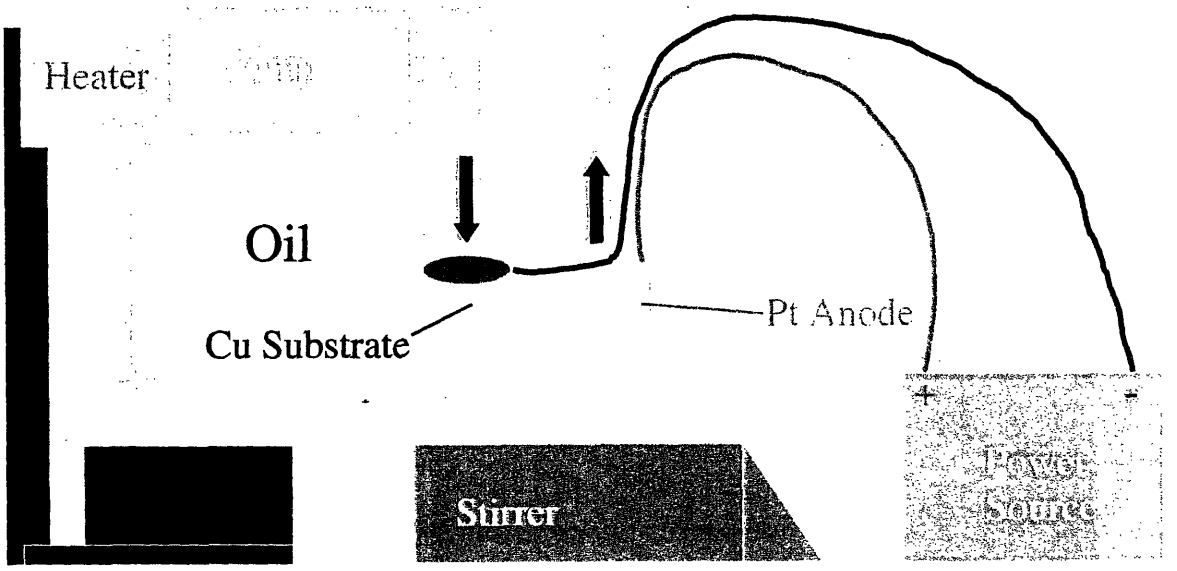

Figure 3: Flow Method Schematic

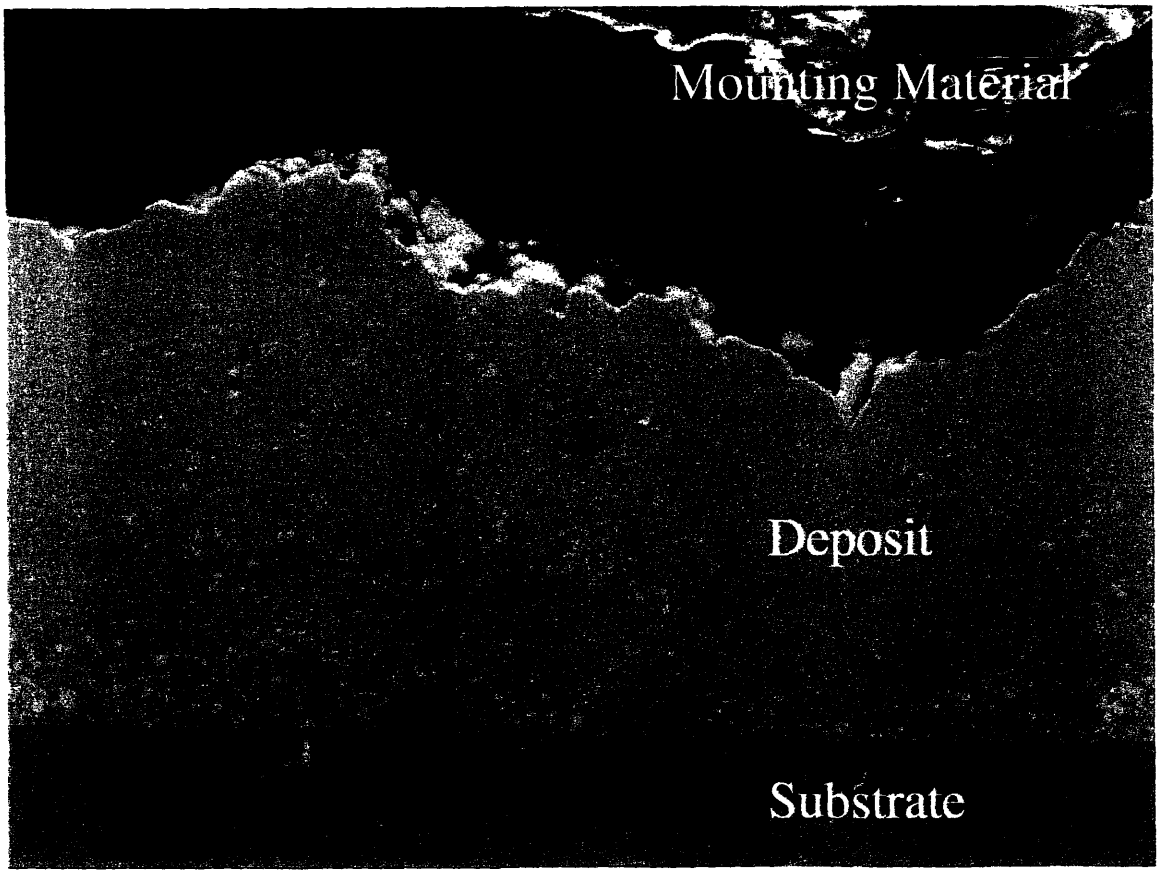

Figure 4: 5g/L Normally Deposited Cross-section

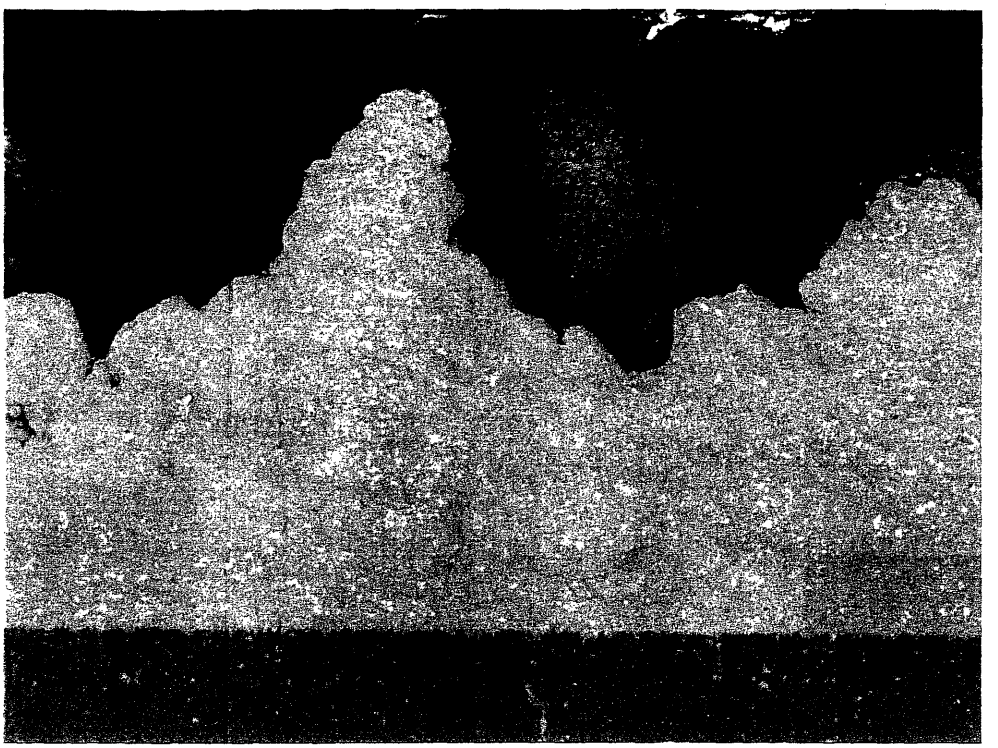

Figure 5: 7.5g/L Normally Deposited Cross-section

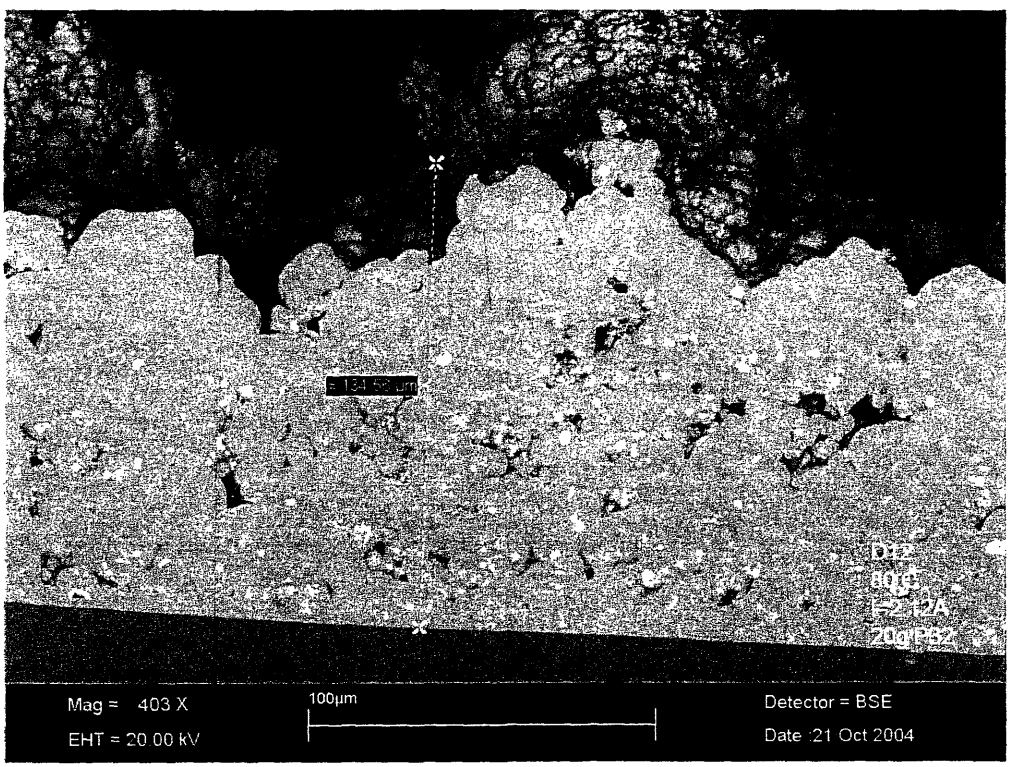

Figure 6: 10g/L Normally Deposited Cross-section

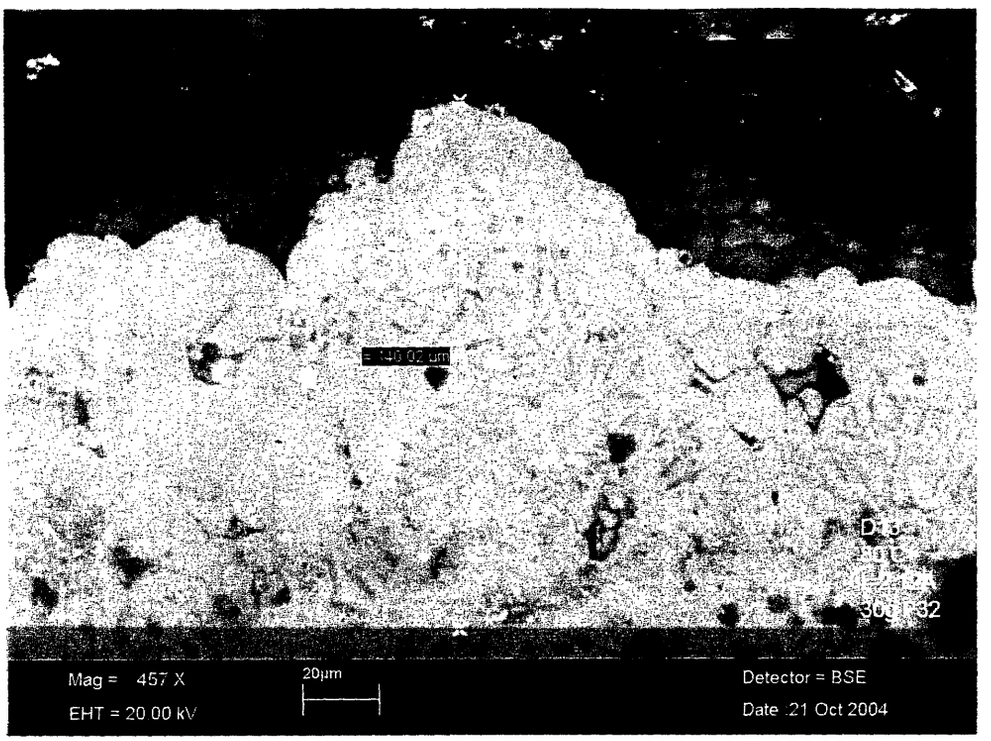

Figure 7: 15g/L Normal Deposited Cross-section

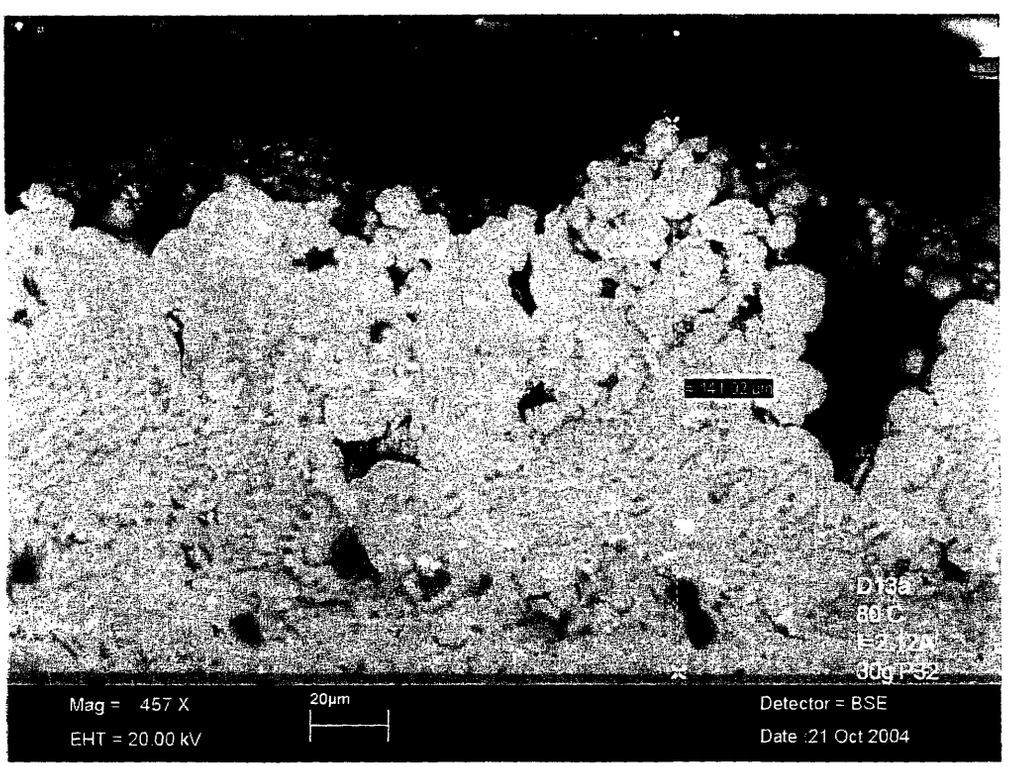

Figure 8: 15g/L Normal Deposited Cross-section

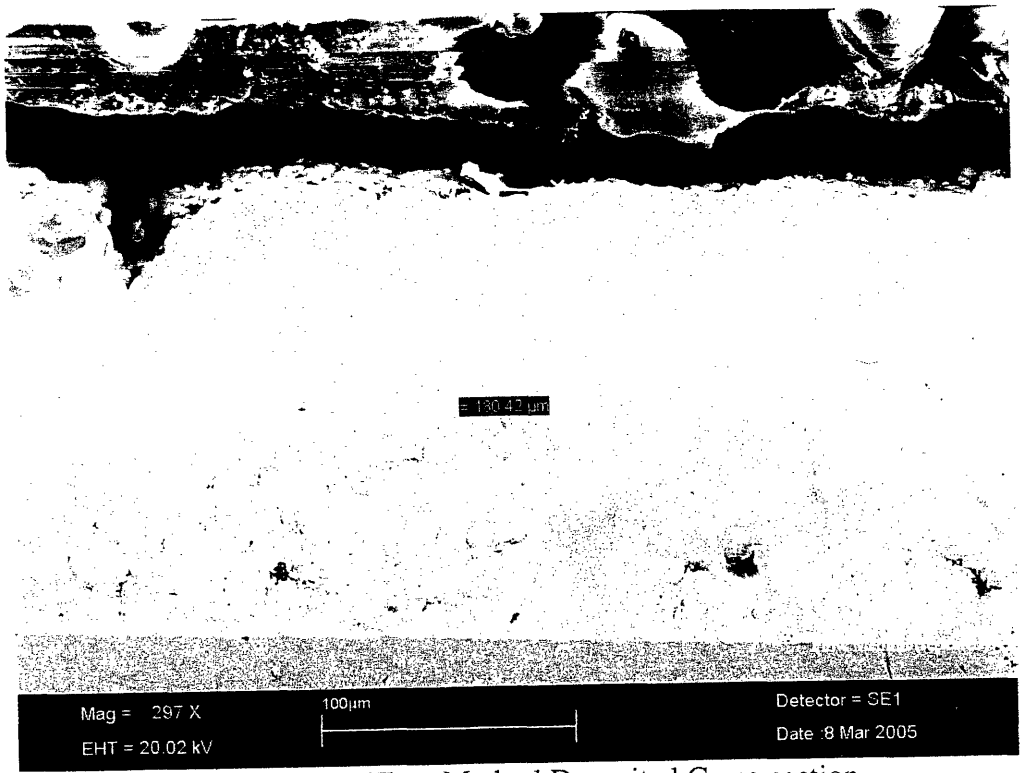

Figure 9: 5g/L Flow Method Deposited Cross-section

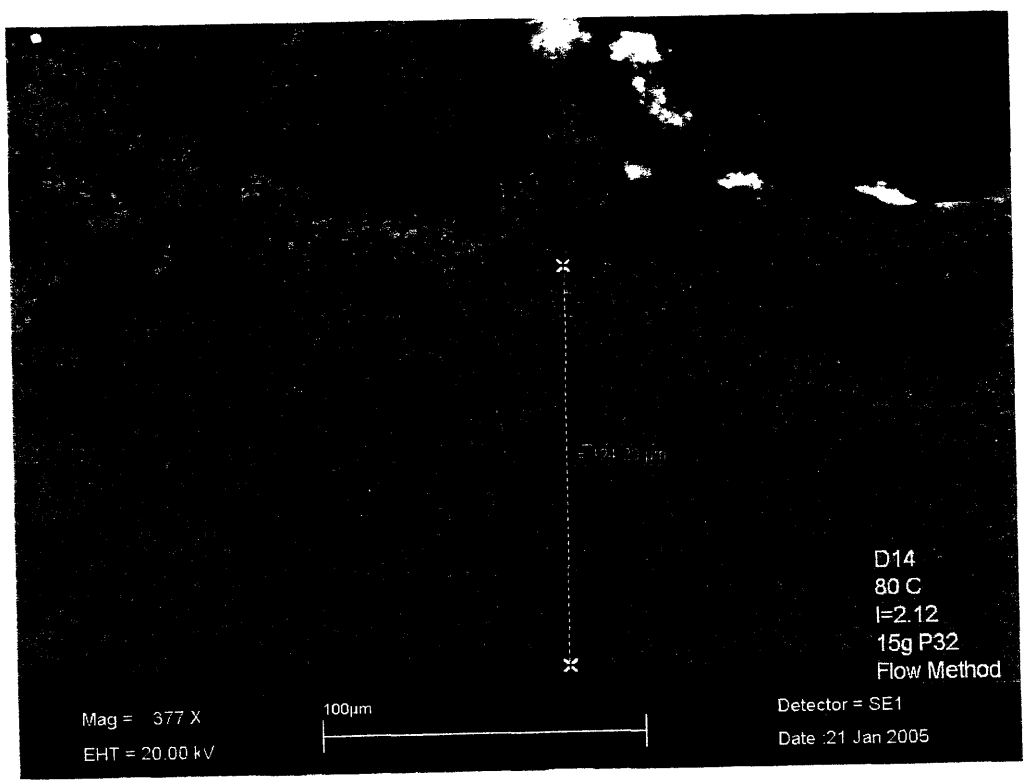

Figure 10: 7.5g/L Flow Method Deposited Cross-section

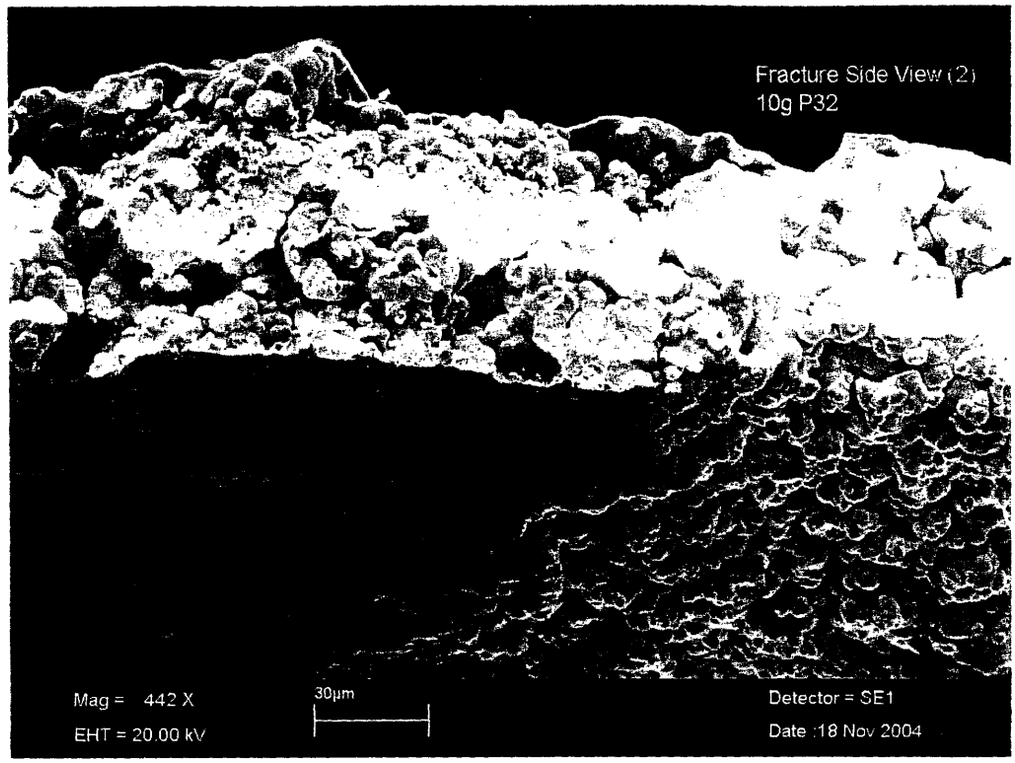

Figure 11: 5g/L Normally Deposited Fracture Surface

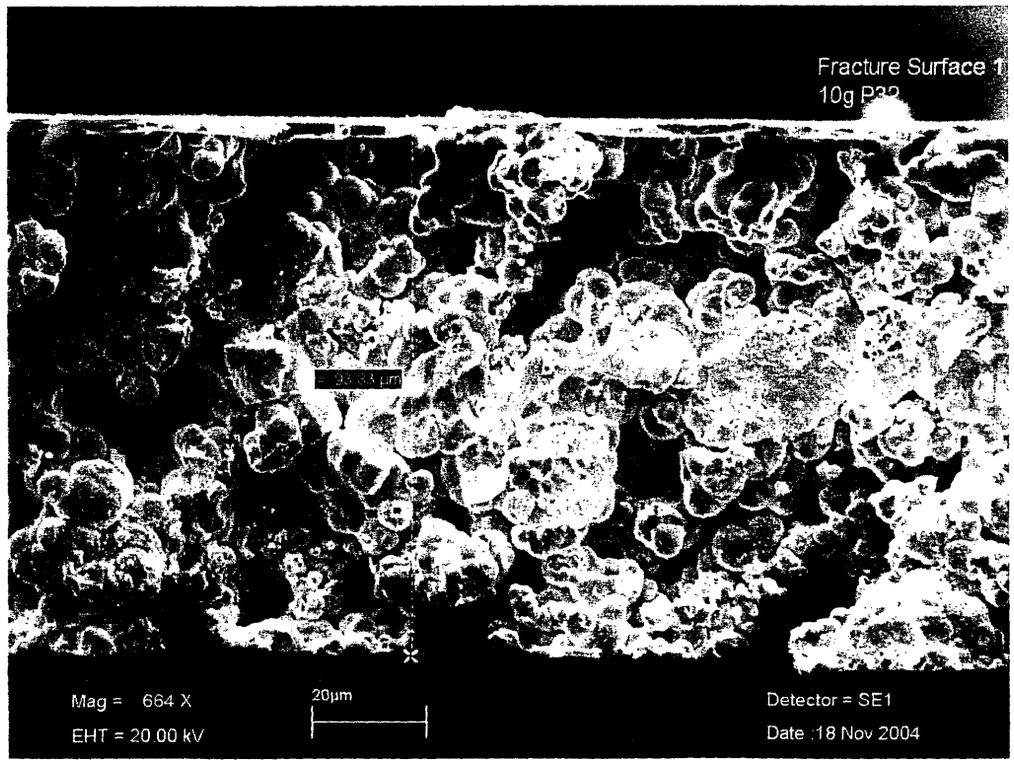

Figure 12: 5g/L Normally Deposited Fracture Surface (Top view)

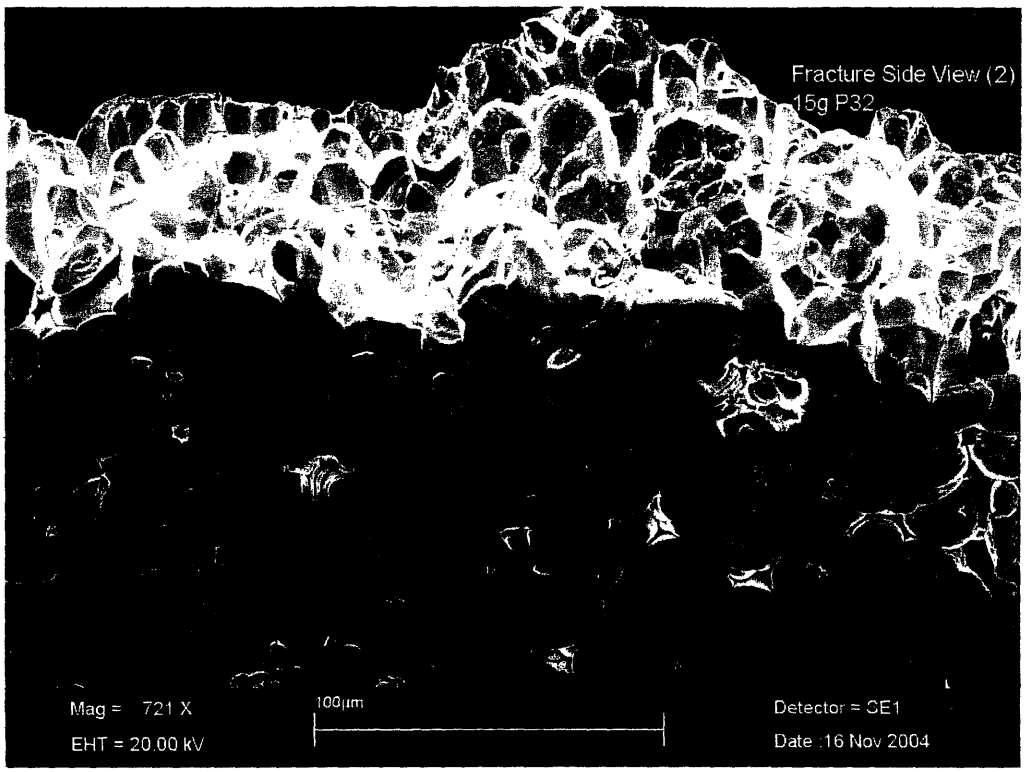

Figure 13: 7.5g/L Normally Deposited Fracture Surface

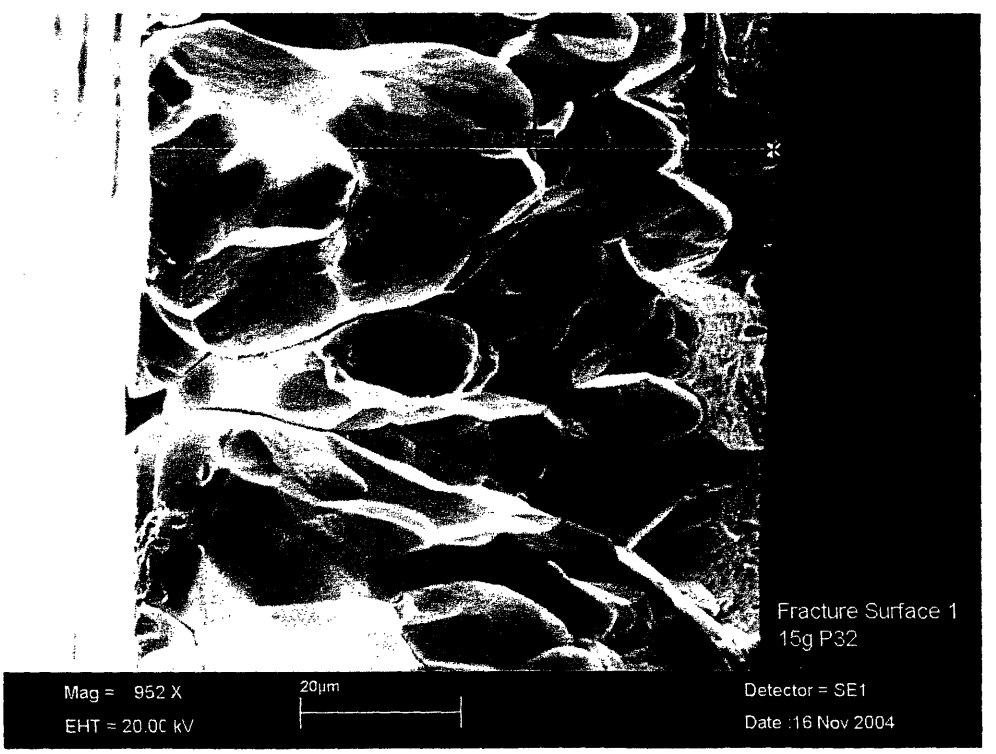

Figure 14: 7.5g/L Normally Deposited Fracture Surface (Top view)

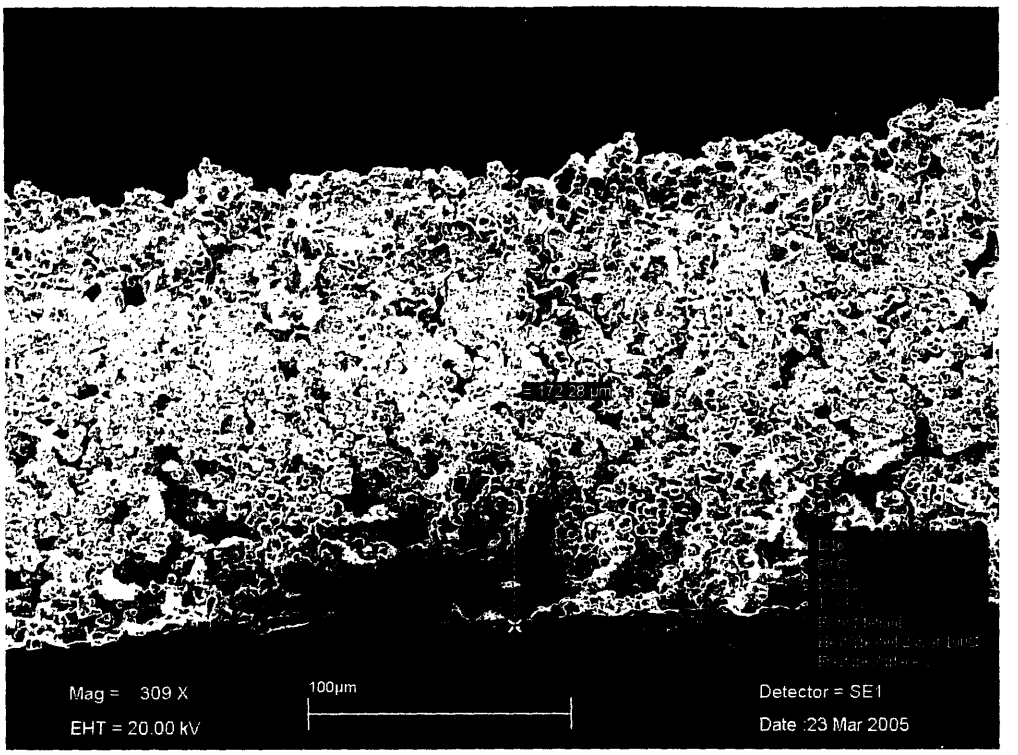

Figure 15: 5g/L Flow Method Deposited Fracture Surface

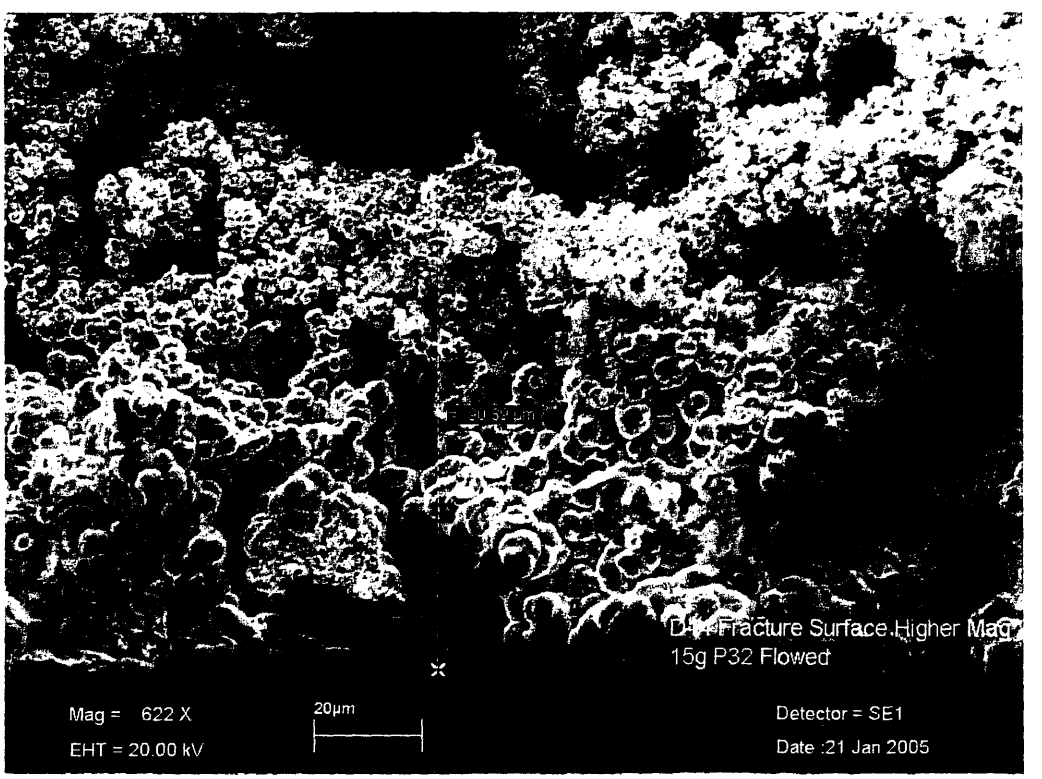

Figure 16: 7.5g/L Flow Method Deposited Fracture Surface

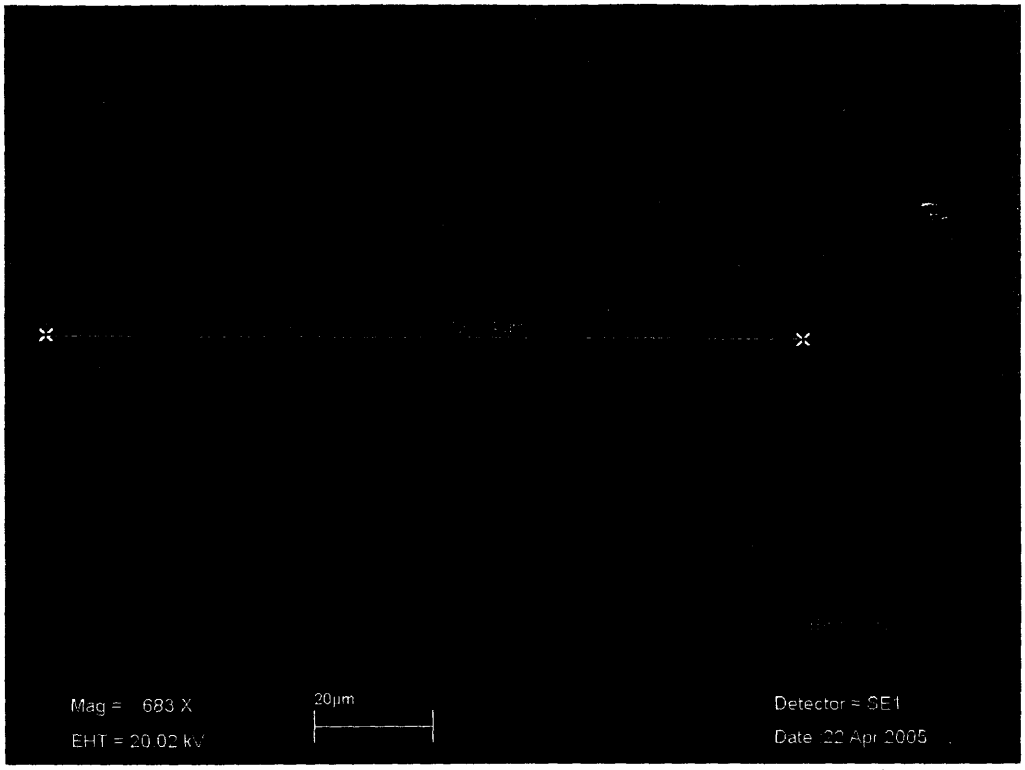

Figure 17: 5g/L Flow Method Deposited Hardness Test (Near Substrate)
Hardness = 1.08 MPa

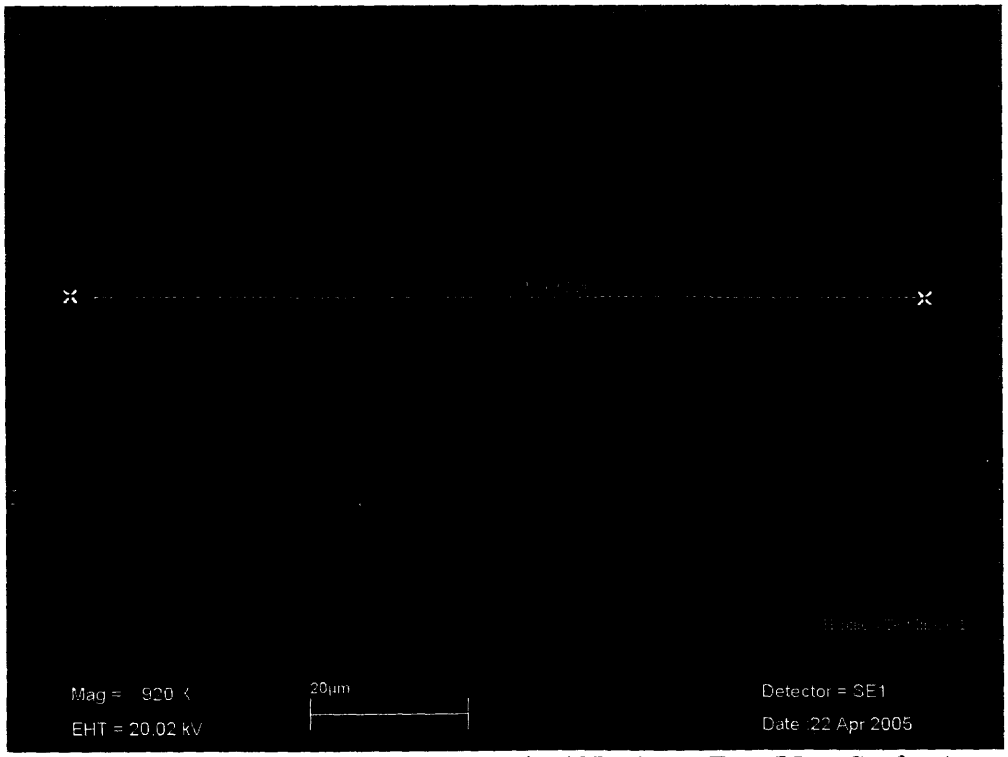

Figure 18: 5g/L Flow Method Deposited Hardness Test (Near Surface)
Hardness = 5.55 MPa

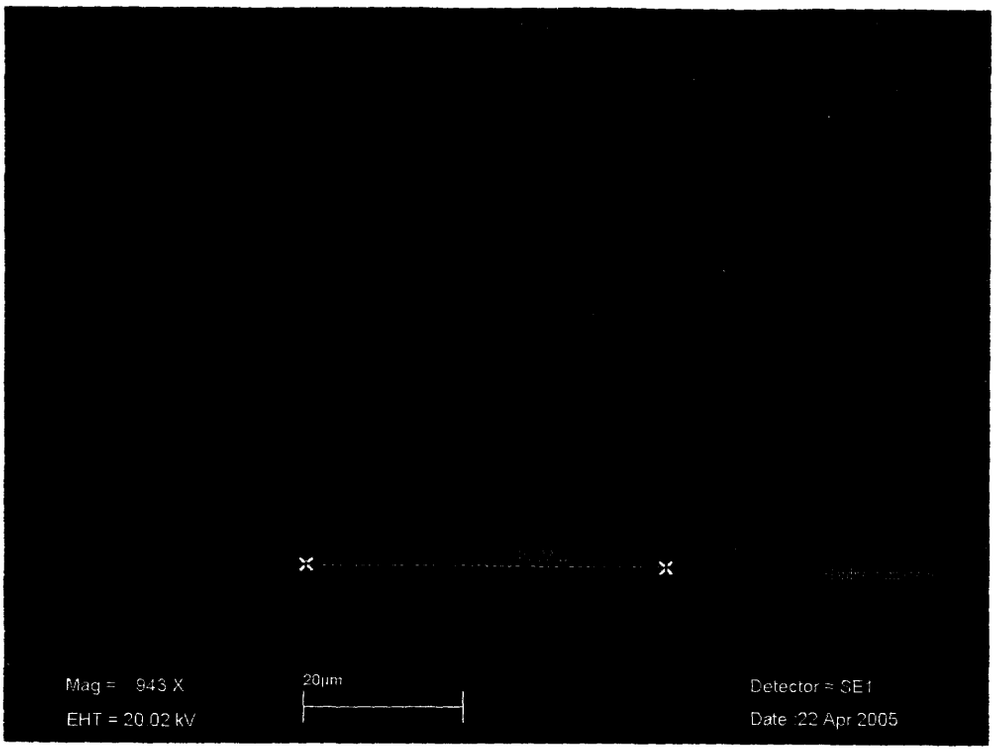

Figure 19: 5g/L Flow Method Deposited Hardness Test with Cracking

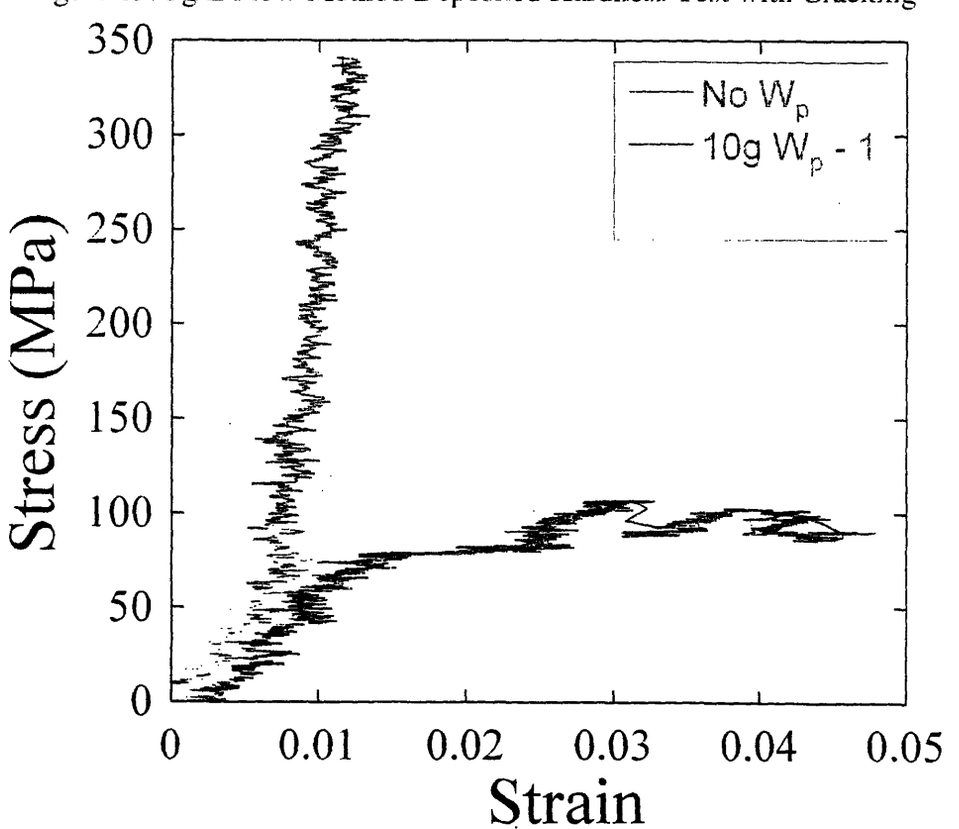

Figure 20: Stress vs. Strain Plots for Compression Samples

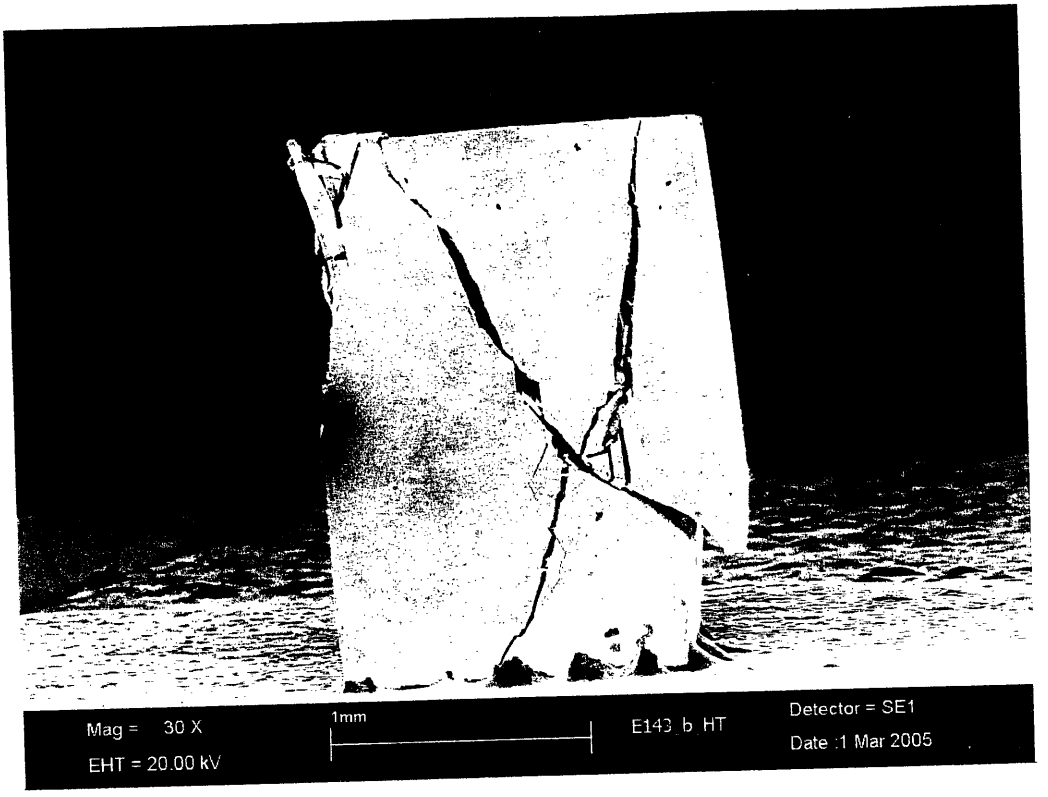

Figure 21: No W_p Compression Result

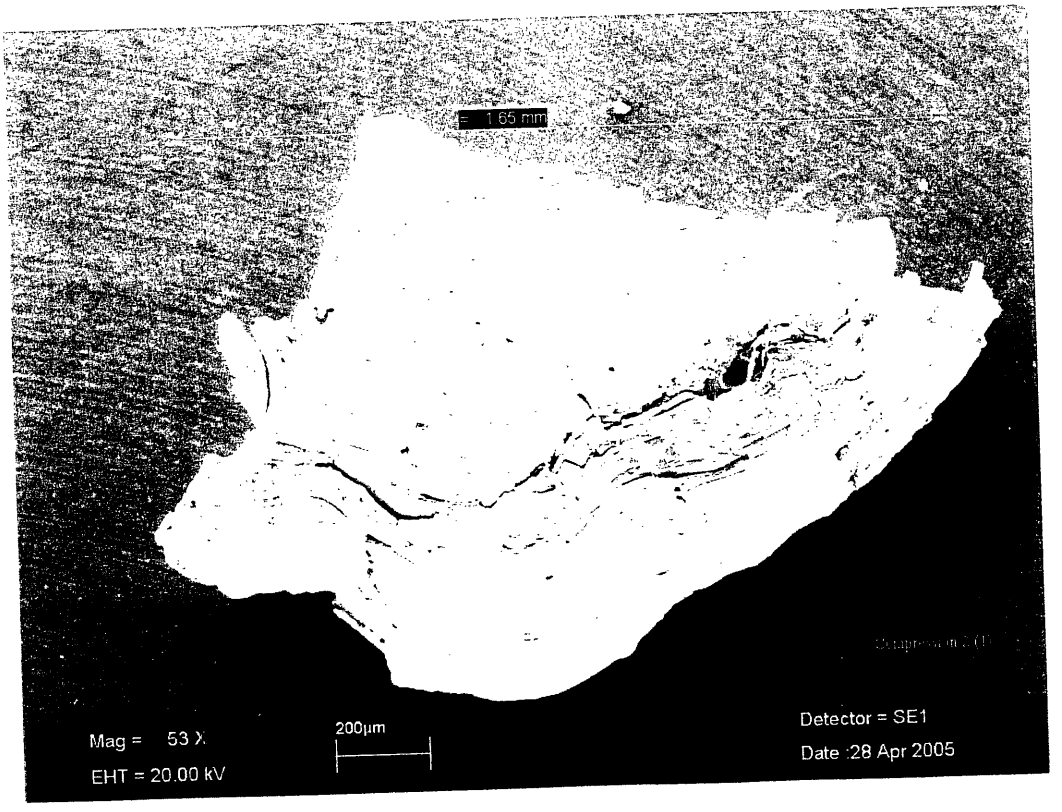

Figure 22: 5g/L Flow Method Deposited 1st Compression Result (Top view)

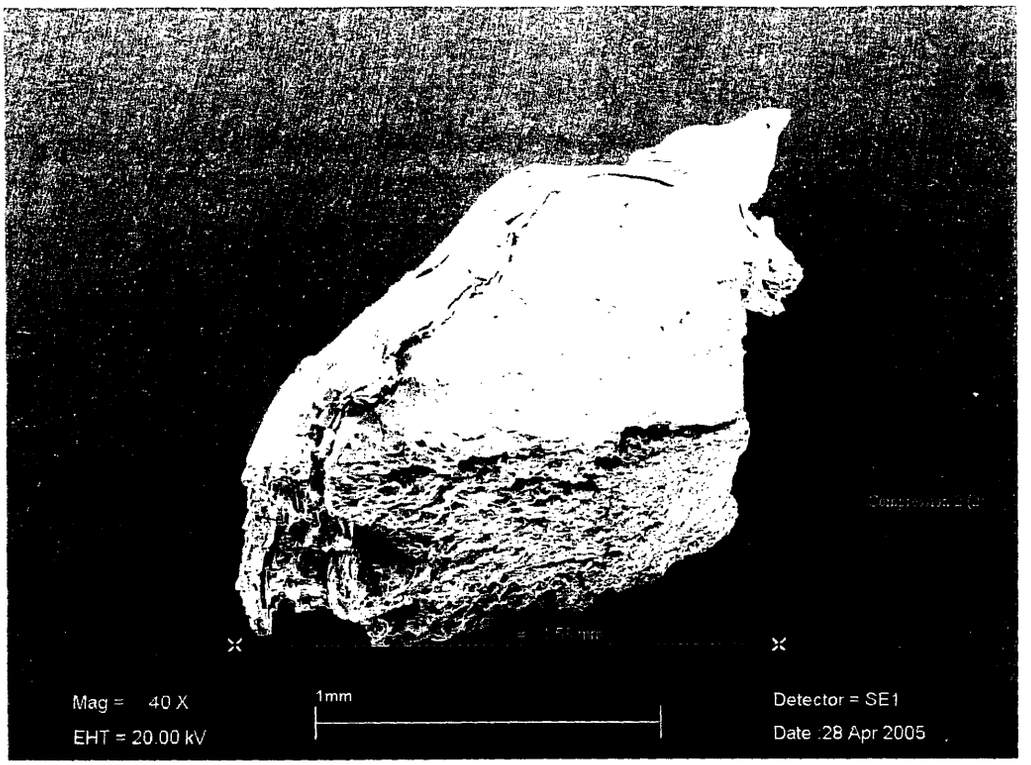

Figure 23: 5g/L Flow Method Deposited 1st Compression Result (Angled view)

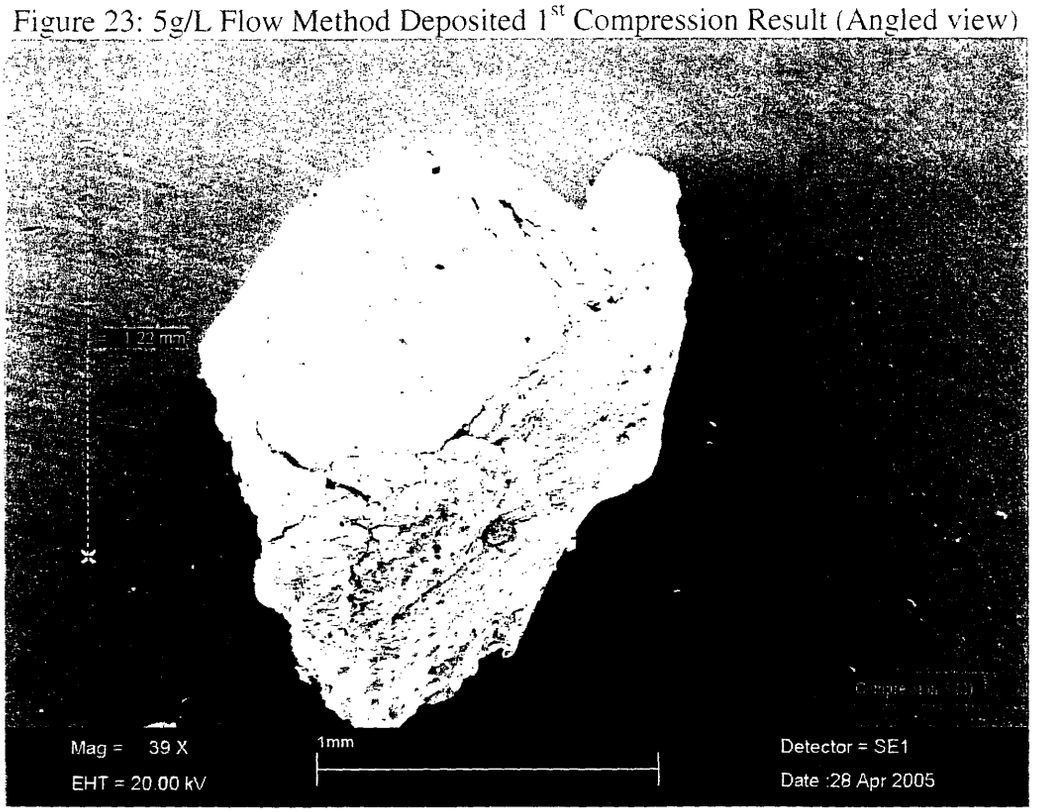

Figure 24: 5g/L Flow Method Deposited 2nd Compression Result (Top view)

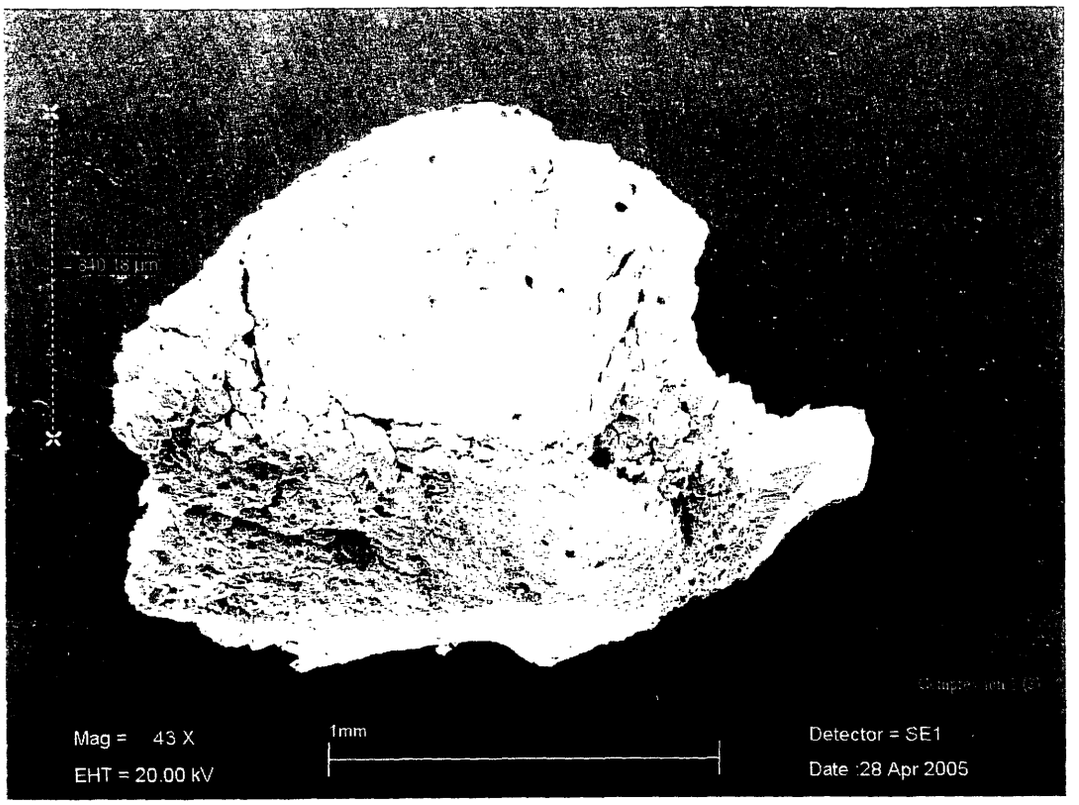

Figure 25: 5g/L Flow Method Deposited 2nd Compression Result (Angled view)